Magnetic field effects on optical and transport properties in InAs/GaAs quantum dots

M. Larsson,* E. S. Moskalenko,† L. A. Larsson, and P. O. Holtz
Department of Physics, Chemistry and Biology (IFM), Linköping University, S-581 83 Linköping, Sweden

C. Verdozzi and C.-O. Almbladh
Solid State Theory, Institute of Physics, Lund University, S-22362 Lund, Sweden

W. V. Schoenfeld and P. M. Petroff
Materials Department, University of California, Santa Barbara, California 93106, USA
(Received 11 January 2006; revised manuscript received 14 June 2006; published 12 December 2006)

A photoluminescence study of self-assembled InAs/GaAs quantum dots under the influence of magnetic fields perpendicular and parallel to the dot layer is presented. At low temperatures, the magnetic field perpendicular to the dot layer alters the in-plane transport properties due to localization of carriers in wetting layer (WL) potential fluctuations. Decreased transport in the WL results in a reduced capture into the quantum dots and consequently a weakened dot-related emission. The effect of the magnetic field exhibits a considerable dot density dependence, which confirms the correlation to the in-plane transport properties. An interesting effect is observed at temperatures above approximately 100 K, for which magnetic fields, both perpendicular and parallel to the dot layer, induced an increment of the quantum dot photoluminescence. This effect is ascribed to the magnetic confinement of the exciton wave function, which increases the probability for carrier capture and localization in the dot, but affects also the radiative recombination with a reduced radiative lifetime in the dots under magnetic compression.

DOI: 10.1103/PhysRevB.74.245312 PACS number(s): 73.21.La, 73.63.Kv

I. INTRODUCTION

The injection of electrons and holes into self-assembled quantum dots (QDs) can be achieved by optical or electrical means. In many applications of QDs, there are requirements of an effective and/or accurate carrier supply to the dot. Due to the small volume and the discrete energy level structure of a QD, the weak absorption of the ground and excited states is often insufficient to be used in practice, i.e., the QD suffers from a small effective absorption cross section. It is often more efficient to make use of the significantly higher absorption in the bulk material and in the wetting layer (WL). In that case, the lateral transport properties of the carriers become important since this transport will determine the effectiveness of the carrier supply to the dot and consequently also the recombination rate of the dot. Furthermore, the electrical injection of carriers relies also on the carrier transport in the surrounding material. In order to control the carrier population in the QDs, the transport properties of carriers in the vicinity of the dot are accordingly important. The lateral transport of carriers has been observed to be affected by several different mechanisms, such as trapping of carriers into WL localization potentials[1,2] or into nonradiative centers in the WL and in the surrounding material.[3,4] Even carrier hopping between the QDs has been demonstrated by employing time-resolved measurements.[5]

In the present work, optical and in-plane transport properties of photoinduced carriers in InAs/GaAs QD structures are studied. A magnetic field perpendicular to the WL alters the carrier transport and capture, which is monitored by changes in the photoluminescence (PL) intensity of the WL versus the dots. A wide temperature range is investigated and the experimental data demonstrate a striking difference between the effect of the magnetic field at low and high temperatures. At low temperatures, the magnetic field reduces the QD related PL intensity, while a significant magnetic field enhanced PL intensity is observed at temperatures above $\approx$100 K. The effect of the applied field is shown to be as strongest in the sample of lowest dot density, in agreement with our model proposed, suggesting that a limiting factor for the dot-related PL is based on the fact that the magnetic field localizes the carriers in WL potential fluctuations.

II. EXPERIMENTAL DETAILS

The InAs/GaAs self-assembled QDs were grown by molecular-beam epitaxy in the Stranski-Krastanov growth mode. After an initial growth of a 100 nm GaAs layer, the dots were formed from a 1.7-monolayer-thick InAs deposition, resulting in approximately 4–5-nm-high and 35-nm-wide QDs on a thin InAs wetting layer (WL). The InAs layer was grown without rotation of the substrate, which results in a gradient of the InAs deposition and consequently a gradient of the QD density. Subsequently, a 100 nm GaAs layer was grown in order to cap the InAs dots. Due to the gradient of the dot density across the wafer, it was possible to study sample pieces with different interdot distance. The dot densities were not accurately determined; instead, we used the ratio between the luminescence intensities of the QDs and WL for a comparison of the dot densities between the different sample pieces.

The magneto-PL measurements were performed in a variable temperature He-cooled cryostat with a superconducting magnet supplying magnetic fields up to 14 T. In the magnetic field dependent measurements, the field was applied along (Faraday geometry), or perpendicular to (Voigt geometry), the normal to the QD layer. The optical access to the

sample, both the optical excitation as well as the collection of the luminescence, was provided by the same multimode optical fiber. A Ti-sapphire laser was used as excitation source, which was tunable between 700 and 1000 nm. The excitation power was kept sufficiently low to excite just the ground state of the QDs. Two different setups were used to detect the PL signal: Either a 0.85-m double-grating monochromator together with a LN_2-cooled Ge detector, using standard lock-in technique, or a single-grating 0.45-m monochromator combined with an LN_2-cooled Si CCD camera.

III. RESULTS AND DISCUSSION

During the growth of QDs in the Stranski-Krastanov mode, variations in alloy composition and strain will cause potential fluctuations in the WL.[1,2] These shallow 2D-like potential fluctuations are able to trap carriers with sufficiently low thermal energy. Consequently, the photoexcited carriers that move along the plane of the WL will have a certain probability to be localized in such potential fluctuations and subsequently recombine if there is a carrier of opposite charge in the vicinity, contributing to the WL emission. Any potential fluctuation will give rise to a locally attractive potential for a charge carrier with a binding energy determined by the thickness and the lateral extension of the fluctuation.[6]

Besides the probability to be captured into a QD or to recombine radiatively in the WL, the carriers may be trapped by a nonradiative recombination center (NRC) in the bulk or in the WL.[3,4] In the following discussion, we will regard NRCs as randomly distributed in the structure. The carrier velocity, mobility, and probability for trapping in a WL potential fluctuation as well as the dot density determine the probability for a carrier to be captured into a QD. Accordingly, if the distance between the dots is smaller than the diffusion length of the carriers, a major part of the electrons will be captured into the dots.

A. Low-temperature photoluminescence

Figure 1 shows the low-temperature PL spectra of the QD and WL for two samples that reveal different dot densities. The low dot density sample exhibits a strong WL emission at 1.44 eV and a QD-related emission centered at 1.27 eV. The spectrum of the corresponding high dot density sample is dominated by a QD emission around 1.24 eV and reveals only a weak WL contribution.

In samples with a high density of QDs, the majority of the carriers will be captured into a QD and recombine, resulting in an intense QD related emission, while the WL PL intensity is weak, or nondetectable (see Fig. 1). The distance between the dots is consequently smaller than the diffusion length of the photoinduced carriers. Our previous study revealed an exciton diffusion length in the WL of approximately 1 μm.[7] Since only a very limited WL contribution can be observed in the low-temperature PL spectrum, we roughly estimate a dot separation of about 1 μm and a dot density of approximately 10^8 cm^{-2}.

In the low dot density sample, the distance between the QDs is larger and there is accordingly a higher probability for the carriers to localize and recombine at WL fluctuations prior to QD capture. The larger fraction of localized carriers in the WL gives rise to the stronger WL-related emission in Fig. 1. As a consequence of the higher probability of carrier localization in the WL, the QD-related emission is reduced. For samples with even lower density (10^6 cm^{-2}), the ratio between the QD and WL integrated intensities is approximately 1%.[8] In our low dot density sample, the ratio is about 50%, which indicates a dot density significantly higher than 10^6 cm^{-2}. The blueshifted QD emission observed for the low dot density sample, in comparison with the high dot density sample, indicates a slightly smaller average dot size and hence a larger quantum confinement shift.

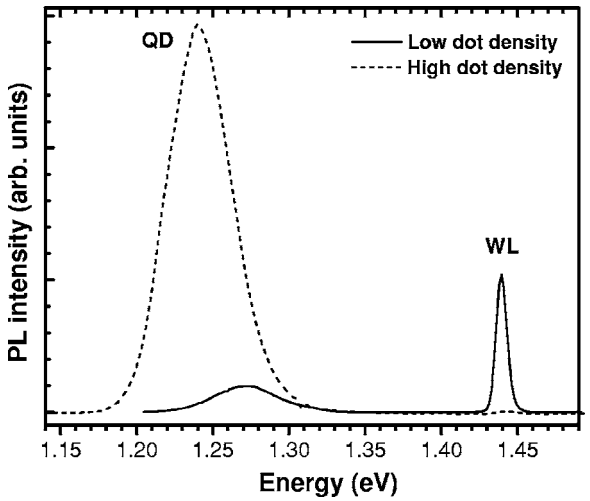

FIG. 1. PL spectra of high and low InAs/GaAs QD density samples, measured at 2 K. The excitation energy was 1.67 eV and the power density was set to 1 W/cm^2.

B. Temperature dependence

In Fig. 2, the integrated intensities of the WL and the QDs

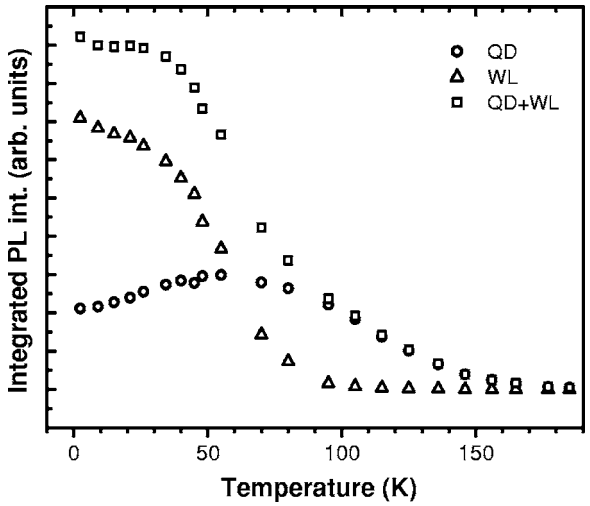

FIG. 2. The temperature dependence on the spectrally integrated PL intensity for the low dot density sample of the QD (circles), WL (triangles), and the total emission (squares).

are plotted as a function of the sample temperature. With increasing temperature, from 2 to 55 K, a reduction of the WL-related emission simultaneously with an enhancement of the QD-related emission is observed. Hence, there is a temperature-induced redistribution of the luminescence intensity from the WL to the QD. However, as the temperature is further increased, also the QD emission is quenched. In the whole temperature range studied, the total PL intensity (of the WL and QDs) monotonously decreases with increased temperature.

For increasing temperatures up to about 55 K, the redistribution of the PL intensity from the WL to the QDs in the low dot density sample is an effect of the increased diffusion length at increased temperatures. Many studies have shown that increased temperatures (up to a certain temperature) will cause an increase of the radiative recombination time in two-dimensional quantum structures.[9–12] Feldmann *et al.*[10] explained the temperature dependence of the decay time in terms of momentum conservation for the free excitons. Since a thermal broadening of the free exciton will reduce the $\mathbf{k}=\mathbf{0}$ exciton population, a smaller fraction of the excitons will fulfill the momentum conservation criteria and an increased exciton lifetime is expected. According to Ridley *et al.*, the thermal equilibrium between free carriers and excitons is predicted to increase the decay time with raised temperature,[13] i.e., thermal ionization of the exciton is taken into account. An increased radiative recombination time for carriers in the WL is expected to result in an increase of the QD-related emission on the expense on the WL PL, as observed experimentally.

Furthermore, increased temperatures also cause delocalization of the carriers from the WL potential fluctuations, which in turn enhances the carrier population and the carrier mobility in the plane of the WL.[11] From the temperature dependence of the WL, shown in Fig. 2, an activation energy of 4 meV can be deduced. Our previous work based on lateral electric field dependence studies on single dot related PL indicates a depth of the potential fluctuations of approximately 3 meV.[14] Furthermore, PLE measurements reveal a Stokes shift of about 5 meV,[7,15] which also gives a rough estimate of the depth of the local WL potential fluctuations. Based on these different experimental observations, the depth of the WL potential fluctuations is estimated to be 3–5 meV.

As a result of the increased decay time and the increased mobility of the carriers, the diffusion length in the plane of the WL increases, which enhances the probability for the carriers to be captured into the QDs. Such an increased transport in the WL also increases the capture probability of the carriers into the NRCs, as reflected by the observed decrease of the total integrated luminescence intensity with increasing temperature. At further elevated temperatures, also other nonradiative recombination processes due to thermal activation of carriers from the WL into the barrier material[12,13,16] and nonradiative recombination at the InAs/GaAs interface[9,17] become significant. As a result, the total integrated PL intensity is further reduced. The thermal activation of nonradiative recombination processes has been demonstrated by the decrease of the radiative decay time at higher temperatures in InAs/GaAs quantum structures.[9,11,12] A negligible PL intensity from the GaAs barrier material is observed in the whole temperature range studied.

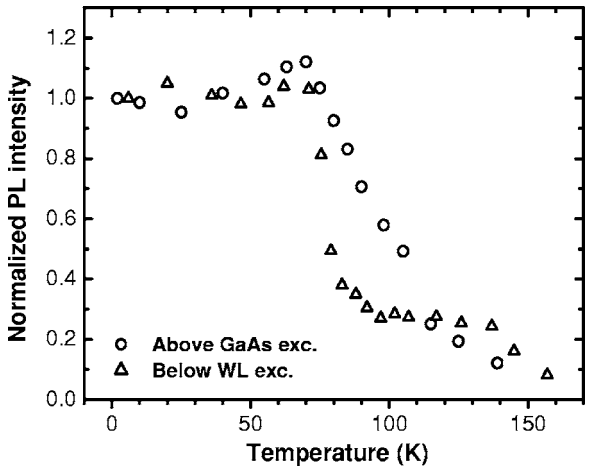

FIG. 3. The temperature dependence on the spectrally integrated PL intensity for the high dot density sample with above (1.67 eV) and below WL (1.37 eV) excitation.

The temperature dependence of the high dot density sample is somewhat different since the WL emission is essentially absent. As seen in Fig. 3, the QD-related luminescence intensity is invariable with temperature up to about 80 K, but decreases for higher temperatures. As discussed above, the capture probability into the QDs is efficient at low temperatures and a majority of the carriers are captured, which results in an intense QD-related emission and a weak or absent WL luminescence. For elevated temperatures, the carrier mobility and diffusion lengths are enhanced in the plane of the WL. However, since there are almost no carriers localized in the WL at low temperatures, almost no increase of delocalized carriers is expected and consequently no increase of the QD emission intensity is observed with increasing temperature. The temperature-induced reduction of the QD emission intensity at temperatures above 80 K is explained in terms of an increased thermal kick out rate from the dots.[18,19] This statement is supported by PL measurements with below WL excitation, where the carriers are excited directly into the dot. PL performed with below and above WL excitation follows the same general temperature dependence. Consequently, the WL transport properties to explain the QD emission intensity variations are hence excluded (Fig. 3). As discussed above, at high temperatures, nonradiative recombination processes become more efficient, which reduce the total luminescence intensity.

C. Magnetic field dependence

Applying a magnetic field perpendicular to the QD layer at low temperatures reduces the intensity of the QD-related emission, as shown in Fig. 4 for the high dot density sample. The integrated WL intensity, on the other hand, exhibits an increase of 13 times when the magnetic field is increased from 0 to 14 T (see the inset of Fig. 4). Similar experimental findings have been reported by Menard *et al.*,[20] who proposed a magnetic field induced change of transport properties causing the PL enhancement.

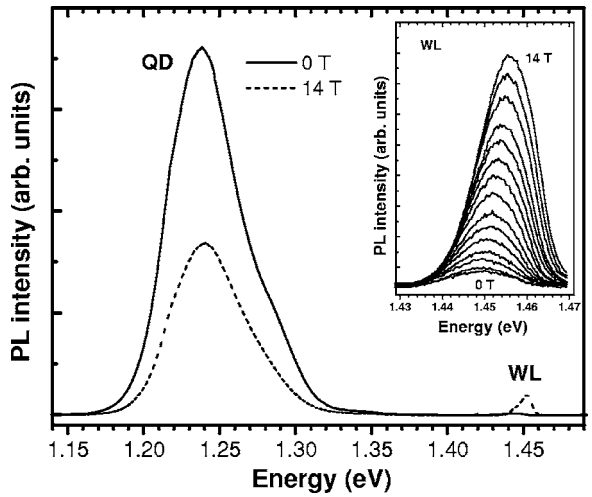

FIG. 4. PL spectrum of a high dot density sample at a temperature of 2 K with an applied magnetic field of 14 T perpendicular to the dot layer, together with a reference spectrum without any applied field. The inset shows the evolution of the WL with increasing magnetic field in steps of 1 T.

A magnetic field perpendicular to the WL compresses the in-plane wave functions of the carriers as predicted by the theory and experimentally indicated by time decay measurements on QWs.[21] Sugawara *et al.*[22] observed an increase of the emission intensity of 1.5 times, in an InGaAs/InP QW, with an applied magnetic field of 7 T, which was ascribed the magnetic field induced compression of the wave function and corresponding increased oscillator strength. In addition to the fact that the magnetic confinement of the carrier wave function increases the oscillator strength in the WL, the field also increases the localization of carriers in the WL potential fluctuations in our case.

D. Electron and hole fluxes

The role of the free carriers can be illustrated in terms of a simple model of semiclassical transport, where the electron and hole motion is assumed to occur in the WL plane. Impurity-induced and external electric fields are in the WL plane, while the external magnetic field is perpendicular (along the positive z axis) to the WL. We consider one Boltzmann's equation for each carrier. While formally independent, these two equations are coupled via the screened electric field. The screening is due to a dielectric constant computed self-consistently in (linear) response[23] to both negative and positive carriers.

Similarly, the current flux through the quantum dot is due to both electrons and holes. To illustrate the procedure, we consider explicitly the case of electrons with charge $-e$. For holes, the treatment follows identically, with $-e \to e$. We start with the standard Boltzmann's equation in real space, in order to evaluate the electron probability distribution $f(\mathbf{r},\mathbf{k})$.[24] Once linearized in the electric field, for constant electric and magnetic fields, the problem is a well known textbook case, as for instance described in Ziman's book.[25] Here the complication is due to the inhomogeneity of the electric field, produced by the randomly distributed charged impurities. In this case, once (i) linearized in the electric field, (ii) in the relaxation-time approximation, and (iii) expressed in the $\mathbf{q}$ space (which is dual to the $\mathbf{r}$ space), Boltzmann's equation for an electron with effective mass m becomes

$$\left(i\mathbf{q}\cdot\mathbf{v}+\frac{1}{\tau}\right)f^1 - e\left(\frac{\partial f^0}{\partial \epsilon}\right)\mathbf{E}(\mathbf{q})\cdot\mathbf{v} + \frac{-e}{mc}(\mathbf{v}\times\mathbf{B})\cdot\nabla_{\mathbf{v}}f^1 = 0. \tag{1}$$

Here $\mathbf{v}=\hbar\mathbf{k}/m$, ϵ is the semiclassical particle energy, τ is the relaxation time, $\mathbf{E}(\mathbf{q})$ is the total (impurity and screening from electrons and holes) field, self-consistently determined at the linear-response level, and $\mathbf{B}$ is the magnetic field along the z axis. Setting $f^1 = e\tau\left(\frac{\partial f^0}{\partial \epsilon}\right)E(\mathbf{q})\varphi(\mathbf{q},\mathbf{k})$, and moving to polar coordinates $\varphi(\mathbf{v}) \to \varphi(v,\theta)$, one gets

$$(i\tau q v\cos\theta + 1)\varphi - v\cos\theta + (\omega_c\tau)\frac{\partial\varphi}{\partial\theta} = 0, \tag{2}$$

where $\omega_c = eB/mc$ is the cyclotron frequency. The idea of incorporating the symmetry (in our case cylindrical) to simplify Boltzmann's equation is not a new one, and has been considered several times in the past (for a recent discussion, see, for example, Ref. 26). Equation (2) is an ordinary differential equation in θ with v as a parameter, and can be solved by quadrature. Alternatively, the required periodic solutions can be obtained by expanding φ in a Fourier series. This leads to a 3-step recursion for the Fourier coefficients, which can be efficiently handled via continued fractions. The expansion in Fourier coefficient has been used previously (see for example Ref. 27). To efficiently handle the three-step recursion for the Fourier coefficients, we use a continued fraction approach. Continued fractions are a well known tool in electronic-structure calculations[28] and formally, our problem is similar to that of an electron moving on a 1D tight-binding chain in the presence of an external electric field.[29] The final explicit expression for the current in real space for a set of impurity charges $\{Q_{\mathbf{R}}\}$ located at positions $\{\mathbf{R}\}$ is

$$\mathbf{J}(\mathbf{r}) = \sum_{\mathbf{R}} [j_{u_{\mathbf{R}}}\hat{\mathbf{u}}_{\mathbf{R}} + j_{v_{\mathbf{R}}}\hat{\mathbf{v}}_{\mathbf{R}}], \quad u_{\mathbf{R}} = |\mathbf{r}-\mathbf{R}|, \quad \hat{\mathbf{u}}_{\mathbf{R}} = \frac{\mathbf{r}-\mathbf{R}}{|\mathbf{r}-\mathbf{R}|}, \tag{3}$$

$$\hat{\mathbf{v}}_{\mathbf{R}} = \hat{\mathbf{z}}\times\hat{\mathbf{u}}_{\mathbf{R}},$$

$$\begin{bmatrix} j_{u_{\mathbf{R}}} & j_{v_{\mathbf{R}}} \end{bmatrix} = Q_{\mathbf{R}}\sigma_0\int_0^\infty dq q\epsilon^{-1}(q)J_1(qu) \times \int_0^\infty du \begin{bmatrix} F_L(x_q u) \\ F_T(x_q u) \end{bmatrix} u e^{-u}, \tag{4}$$

where $\epsilon(q)$ is the dielectric constant (from both electrons and holes), J_1 is the integer Bessel function, $\sigma_0 = e^2\tau n_0/m$, and $x_q = \frac{2\tau^2 q^2}{\beta m}$ (β is the inverse temperature). On the right-hand side of Eq. (4), the subscript in $u_{\mathbf{R}}$ has been dropped to alleviate the notation. Finally, the recursive character of the solution enters via

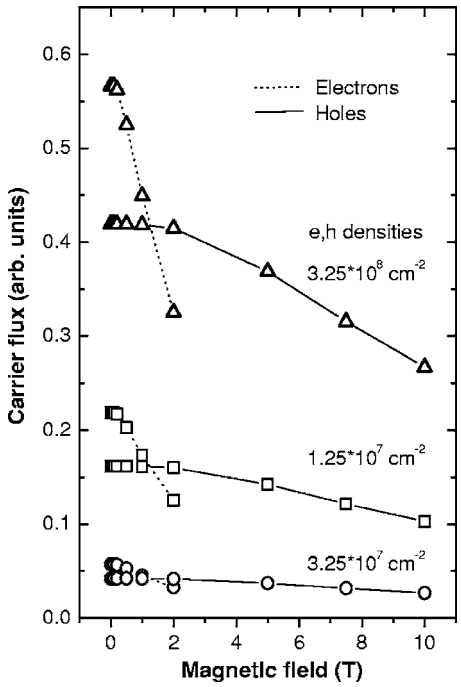

FIG. 5. Predicted electron and hole fluxes into a single QD as a function of a magnetic field perpendicular to the dot layer, as achieved from the model employed.

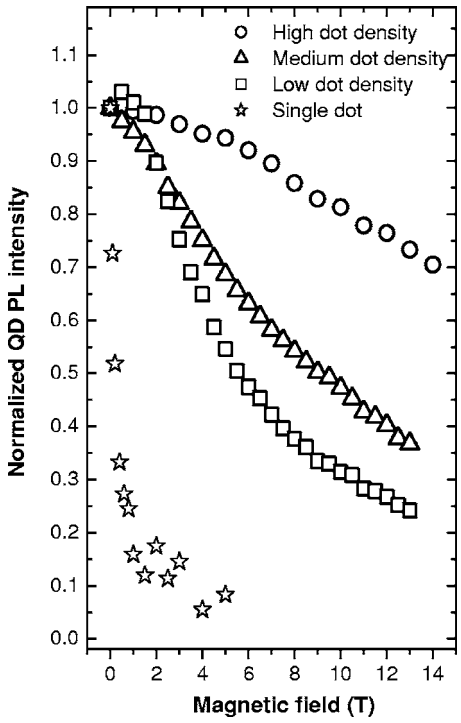

FIG. 6. The magnetic field dependence in Faraday geometry of the integrated QD PL intensity at 2 K for three different dot densities together with a single dot. The PL intensity of each sample is normalized to the intensity of the emission at zero field.

$$F_L(x) = \frac{2\,\mathrm{Re}[\tilde{A}(x)]}{1 + x\,\mathrm{Re}[\tilde{A}(x)]}, \quad F_T(x) = \frac{-2\,\mathrm{Im}[\tilde{A}(x)]}{1 + x\,\mathrm{Re}[\tilde{A}(x)]}, \quad (5)$$

$$\tilde{A}(x) = \cfrac{1}{w_1 - \cfrac{x}{w_2 - \cfrac{x}{w_3 - \cdots}}}.$$

In these expressions, the dependence on B shows only in $(\omega_c\tau)$. The latter in turn appears only in the coefficients $w_n = 2(1 + in\omega_c\tau)$ in $\tilde{A}(x)$. We wish to restate at this point that there is one such solution for each carrier type, Eqs. (3)–(5). Formally, they are obtained one from the other by interchanging $-e \leftrightarrow e$. However, the two solutions are coupled via the screening response (from both electrons and holes) in the WL. A treatment of the screened response along similar lines can be found in Ref. 30.

The flux through the dot, to be related to the carrier photorecombination, is determined by considering the carriers crossing the dot boundary. The dot is assumed to be circular in shape with radius R_D and centered at the origin of the xy plane. The drain of carriers in the dot is simulated by retaining only the ingoing contribution, namely (Θ is the Heavside function)

$$\Phi_J = \oint_{\text{positive}} d\vec{l} \cdot \mathbf{J} = R_D \int_0^{2\pi} d\phi\, \hat{\mathbf{n}}_\phi \cdot \mathbf{J}(r,\phi)\Theta(\hat{\mathbf{n}} \cdot \mathbf{J}), \quad (6)$$

where $\hat{\mathbf{n}}_\phi = (-\cos\phi, -\sin\phi)$ determines the ingoing direction for the current $\mathbf{J}$, calculated on the circle of radius R_D, i.e., on the dot boundary. In Eq. (6), $\mathbf{J}$ represents the total $e+h$ current due to the (impurity-related and external) electric and external magnetic fields.

In Fig. 5, the results for the electron and hole fluxes Φ at different particle concentrations are shown, as a function of the external magnetic field, for a fixed temperature ($T = 300$ K). The results refer to a single dot geometry, with in-plane, randomly distributed charged impurities. The decrease of the flux with increasing field is apparent.

Accordingly, the carrier flux to the dot will decrease with increasing magnetic field, which decreases the probability for the carriers to be captured into the QDs. As a result, a redistribution of carriers from the QDs to the WL is expected to reduce the QD emission, which is accompanied by an increase of the WL PL intensity, in agreement with the experimental results (see Fig. 4).

The strength of the magnetic field induced PL intensity enhancement effect is shown to be dot-density-dependent. As seen in Fig. 6, the emission intensity from the QDs in the low dot density sample is reduced by four times when the magnetic field is increased up to 14 T, while a decrease of only 1.5 times was observed for the sample with the high dot density. In samples with a low dot density, the effect with a PL intensity decrease for the QDs for increasing magnetic field is stronger than in samples with a high dot density (see Fig. 6). In a sample with a low dot density, the number of WL localization potentials is larger relative to the number of dot potentials than in samples of high dot density. Since the magnetic field increases the probability for localization at each localization potential, the effect of the magnetic field on

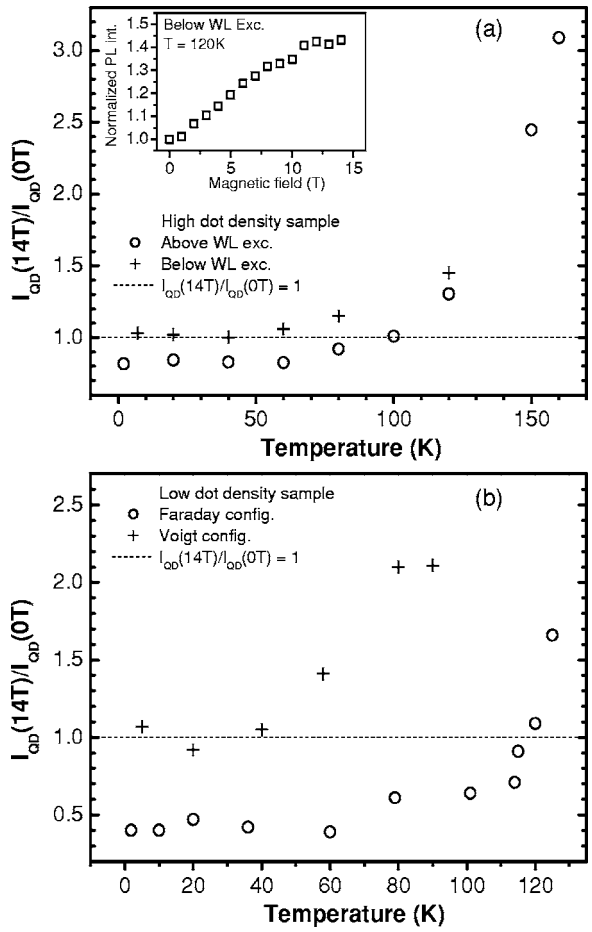

FIG. 7. (a) The ratio of the integrated dot PL intensity between 14 and 0 T in Faraday geometry of the high dot density sample as a function of temperature under excitation with above and below WL energy. The inset shows the normalized PL intensity with below the WL excitation as a function of the applied magnetic field, measured at 120 K. (b) The ratio of the integrated dot PL intensity between 14 and 0 T of the low dot density sample as a function of temperature with above WL excitation for Faraday and Voigt geometry.

the QD intensity is accordingly more pronounced in low dot density samples in comparison with high dot density samples. This dependence on the dot density is further established when measuring the effect of the magnetic field for individual dots. In single dot spectroscopy with interdot distances of about 10 μm (Ref. 8) with magnetic fields up to 5 T, a reduction of the QD PL intensity of about 15 times was observed.

E. High-temperature magnetic field dependence

There is a remarkably abrupt enhancement of the magnetic field induced QD luminescence intensity when increasing the temperature above $\approx$100 K. Instead of reducing the QD luminescence intensity as observed for lower temperatures, the magnetic field causes an increase of the QD related PL intensity, as shown in Fig. 7. The magnetic field induced PL enhancement increases with increasing temperatures, to reach a relative enhancement of three times $[I_{QD}(14\ T)/I_{QD}(0\ T) \approx 3]$ at 160 K. This unexpected observation can be explained in terms of a magnetic field enhanced capture: At relatively low temperatures ($50 \leqslant T \leqslant 100$ K), the carriers have a thermal energy, which is sufficient for delocalization from the potential fluctuations without a magnetic field, but when a magnetic field is applied, the carriers get localized in these potential fluctuations. Consequently, the PL intensity of the QDs is reduced (see Fig. 7). However, for temperatures above $\approx$100 K, the thermal energy of the carriers is relatively high and the carriers will not be localized in the WL potential fluctuations even with a magnetic field applied. However, it is expected that the magnetic field can localize carriers in the considerably deeper QD potentials. Consequently, the magnetic field will affect both the carrier *transport* and the *capture* process of the carriers into the dot. The transport is gradually more hindered with increasing field due to progressively stronger localization effects. The field will, on the other hand, enhance the capture process of carriers from the WL into the dots. The experimental observation that the QD PL intensity increases with increasing applied magnetic field at high temperatures implies that the latter effect is the predominant factor for those conditions (see Fig. 7).

For measurements with below WL excitation, any capture process into the dots of carriers created in the WL is absent since the absorption takes place solely in the QDs. As expected, no change of the PL intensity was observed at temperatures below $\approx$80 K with below WL excitation [see Fig. 7(a)]. However, by increasing the temperature above $\approx$80 K, thermal excitation of carriers from the dots becomes significant (as shown in Fig. 3). A magnetic field applied perpendicular to the dot layer, i.e., the Faraday configuration, enhances the recapture of the kicked-out carriers. As a result of such an enhanced recapture, we observe an increasing QD-related luminescence with increasing magnetic field at temperatures above $\approx$80 K and with below WL excitation [see the inset in Fig. 7(a)]. It should be stressed that the magnetic field enhanced capture into the dots is present at all temperatures, but the effect of the carrier localization in WL potentials and the magnetic field reduced flux to the dot are the predominant factors determining the PL intensity at low temperatures.

Also the lifetime of the exciton should be taken into account when considering expected PL intensity variations. As the magnetic field is increased, the lifetime of the exciton in a QD is reduced,[31] giving rise to an increase of the PL intensity. The magnetic field induced compression of the excitonic wave function increases the oscillator strength in quantum structures,[21] as previously mentioned. Even though the exciton wave function is already fairly compressed by the confinement potential of the dot, the magnetic field further enhances the oscillator strength. A decreased decay time of the radiative recombination in QDs with increased magnetic field at low temperatures has earlier been demonstrated by Lomascolo *et al.*[31] This effect is observed to be more pronounced at higher temperatures for our QD system. As discussed above, the carriers in the QD have a certain probability to be thermally excited out of the dot at high temperatures. There is accordingly a competition for the car-

riers to either be kicked out of the dot or to radiatively recombine. By decreasing the radiative decay time with an applied magnetic field, i.e., increasing the probability for radiative recombination, an increased emission efficiency is expected for a magnetic field applied. At above WL excitation, the effect of the decreased decay time at low temperatures is of minor importance since the QD PL intensity in that case is essentially determined by the in-plane transport properties. Both enhanced carrier recapture to the dots and reduction of the radiative lifetime of the carriers in the dots under applied magnetic field are contributing to the dot-related PL intensity increase at high temperatures.

In the Voigt geometry, with the magnetic field applied in parallel to the WL, the transport properties in the WL are expected to be essentially unaffected by the magnetic field. In accordance with these expectations, no change of the QD-related PL intensity was observed in the Voigt configuration at temperatures below ≈ 50 K, as shown in Fig. 7(b). At higher temperatures, the magnetic field is still able to squeeze the electron-hole wave function, which in turn results in an enhanced QD emission rate and intensity, in accordance with the discussion above and the experimental data presented in Fig. 7(b). Since the in-plane transport is not significantly limited by the magnetic field in the Voigt geometry, the ratio between the QD PL intensity at 14 and 0 T is expected to be higher in Voigt than in Faraday geometry, in agreement with the experimental results in Fig. 7(b).

IV. CONCLUSIONS

The effect of a magnetic field perpendicular to the dot layer was studied in a wide temperature range. An observed redistribution of the PL intensity from the QDs to the WL for a magnetic field in the Faraday geometry, i.e., applied perpendicular to the WL, at low temperatures, demonstrates that the in-plane transport is considerably affected. At temperatures below approximately 100 K, the magnetic field in the Faraday geometry reduces the lateral transport to the dots since the field localizes carriers in WL potential fluctuations with a depth of a few meV. A semiclassical Boltzmann equation was considered for both electrons and holes in the presence of a magnetic and an internal electric field to explain the flux of the carriers. Furthermore, the effect of the magnetic field at low temperatures is strongest for low dot densities, in agreement with the localization of carriers in the WL potentials. As predicted, our results show that the in-plane transport properties are not significantly altered by a magnetic field in the Voigt geometry, since the compression of the carrier wave function in the plane of the WL is limited. For temperatures above ≈ 100 K, the magnetic field cannot localize carriers in the WL due to the relatively high thermal energy. However, the magnetic field is able to enhance the localization of carriers in the considerably deeper QD potentials, resulting in an increase of the QD PL intensity with increasing fields for $T \geqslant 100$ K, in both Faraday and Voigt geometry. The reduced exciton lifetime with an applied magnetic field will also contribute to the enhanced QD PL intensity. The effect of the reduced lifetime, however, does not change the QD PL intensity at low temperatures since the thermal kick-out rate of the carriers from the dot is very low and the capture rate is essentially determined by the in-plane carrier transport.

ACKNOWLEDGMENTS

This work was supported by grants from the Swedish Foundation for Strategic Research (SSF) and Swedish Research Council (VR). E.S.M. gratefully acknowledges financial support from the Royal Swedish Academy of Sciences (KVA) and partial support from the program "Low-Dimensional Quantum Structures" of the Russian Academy of Sciences.

*Electronic address: matla@ifm.liu.se
†Permanent address: A. F. Ioffe Physical-Technical Institute, Russian Academy of Sciences, 194021, Polytechnicheskaya 26, St. Petersburg, Russia.

[1] C. Lobo, R. Leon, S. Marcinkevičius, W. Yang, P. C. Sercel, X. Z. Liao, J. Zou, and D. J. H. Cockayne, Phys. Rev. B **60**, 16647 (1999).
[2] R. Heitz, T. R. Ramachandran, A. Kalburge, Q. Xie, I. Mukhametzhanov, P. Chen, and A. Madhukar, Phys. Rev. Lett. **78**, 4071 (1997).
[3] M. M. Sobolev, A. R. Kovsh, V. M. Ustinov, A. Y. Egorov, A. E. Zhukov, M. V. Maksimov, and N. N. Ledentsov, Semiconductors **31**, 1074 (1997).
[4] S. Marcinkevičius, J. Siegert, R. Leon, B. Cechavicius, B. Magness, W. Taylor, and C. Lobo, Phys. Rev. B **66**, 235314 (2002).
[5] A. F. G. Monte, J. J. Finley, A. D. Ashmore, A. M. Fox, D. J. Mowbray, M. S. Skolnik, and M. Hopkinson, J. Appl. Phys. **93**, 3524 (2003).
[6] G. Bastard, C. Delalande, M. H. Meynadier, P. M. Frijlink, and M. Voos, Phys. Rev. B **29**, 7042 (1984).
[7] E. S. Moskalenko, V. Donchev, K. F. Karlsson, P. O. Holtz, B. Monemar, W. V. Schoenfeld, J. M. Garcia, and P. M. Petroff, Phys. Rev. B **68**, 155317 (2003).
[8] E. S. Moskalenko, K. F. Karlsson, V. Donchev, P. O. Holtz, W. V. Schoenfeld, and P. M. Petroff, Appl. Phys. Lett. **84**, 4896 (2004).
[9] M. Gurioli, A. Vinattieri, M. Colocci, C. Deparis, J. Massies, G. Neu, A. Bosacchi, and S. Franchi, Phys. Rev. B **44**, 3115 (1991).
[10] J. Feldmann, G. Peter, E. O. Göbel, P. Dawson, K. Moore, C. Foxon, and R. J. Elliott, Phys. Rev. Lett. **59**, 2337 (1987).
[11] H. Hillmer, A. Forchel, S. Hansmann, M. Morohashi, E. Lopez, H. P. Meier, and K. Ploog, Phys. Rev. B **39**, 10901 (1989).
[12] G. Bacher, C. Hartmann, H. Schweizer, T. Held, G. Mahler, and H. Nickel, Phys. Rev. B **47**, 9545 (1993).
[13] B. K. Ridley, Phys. Rev. B **41**, 12190 (1990).
[14] E. S. Moskalenko, M. Larsson, W. V. Schoenfeld, P. M. Petroff, and P. O. Holtz, Phys. Rev. B **73**, 155336 (2006).

[15] E. S. Moskalenko, K. F. Karlsson, P. O. Holtz, B. Monemar, W. V. Schoenfeld, J. M. Garcia, and P. M. Petroff, Phys. Rev. B **66**, 195332 (2002).
[16] J. D. Lambkin, D. J. Dunstan, K. P. Homewood, L. K. Howard, and M. T. Emeny, Appl. Phys. Lett. **57**, 1986 (1990).
[17] W. Pickin and J. P. R. David, Appl. Phys. Lett. **56**, 268 (1990).
[18] G. Wang, S. Fafard, D. Leonard, J. E. Bowers, J. L. Merz, and P. M. Petroff, Appl. Phys. Lett. **64**, 2815 (1994).
[19] D. I. Lubyshev, P. P. Gonzlez-Borrero, E. Marega, Jr., E. Petitprez, N. La Sacala, Jr., and P. Basmaji, Appl. Phys. Lett. **68**, 205 (1996).
[20] S. Menard, J. Beerens, D. Morris, V. Aimez, J. Beauvais, and S. Fafard, J. Vac. Sci. Technol. B **20**, 1501 (2002).
[21] I. Aksenov, Y. Aoyagi, J. Kusano, T. Sugano, T. Yasuda, and Y. Segawa, Phys. Rev. B **52**, 17430 (1995).
[22] M. Sugawara, N. Okazaki, T. Fujii, and S. Yamazaki, Phys. Rev. B **48**, 8848 (1993).
[23] A. L. Fetter and J. D. Walecka, *Quantum Theory of Many Particle Systems* (McGraw-Hill, New York, 1971).
[24] C. Hamaguchi, *Basic Semiconductor Physics* (Springer, Berlin, 2001).
[25] J. M. Ziman, *Principles of the Theory of Solids* (Cambridge University Press, London, 1965).
[26] H. Date and M. Shimozuma, Phys. Rev. E **64**, 066410 (2001).
[27] P. Hedegård and A. Smith, Phys. Rev. B **51**, 10869 (1995).
[28] D. W. Bullet, R. Haydock, V. Heine, and M. J. Kelly, *Solid State Physics* (Academic, New York, 1980), Vol. 35.
[29] S. G. Davidson, R. A. English, Z. L. Mišković, F. Goodman, A. T. Amos, and B. L. Burrows, J. Phys.: Condens. Matter **9**, 6371 (1997).
[30] B. O. Sernelius and E. Söderström, J. Phys.: Condens. Matter **3**, 1493 (1991).
[31] M. Lomascolo, R. Cingolani, P. O. Vaccaro, and K. Fujita, Appl. Phys. Lett. **74**, 676 (1999).